Edge Detection for Weed Recognition in Lawns

Lorena Parra[1], Jose Marin[2], Salima Yousfi[3], Gregorio Rincón[2], Pedro Vicente Mauri[3], and Jaime Lloret[1,*]

[1] Instituto de Investigación para la Gestión Integrada de Zonas Costeras, Universitat Politècnica de València, 46730 Grao de Gandia, Valencia, Spain, loparbo@doctor.upv.es(L.P.), jlloret@dcom.upv.es(J.L.)
[2] Departamento de Investigación e Innovación, AreaVerde MG projects Madrid, 28050 Madrid, Spain; jmarin@areaverde.es (J.M), rincondlh@hotmail.com(G.R.)
[3] Departamento de Investigación Agroambiental, Instituto Madrileño de Investigación y Desarrollo Rural, Agrario y Alimentario, 28800 Madrid, Spain; salima.yousfi@madrid.org(S.Y.), pedro.mauri@madrid.org(P.V.M.)

* Correspondence: jlloret@dcom.upv.es

Abstract: The rapid propagation of weeds is a major issue for turfgrass management (both ornamental and sports turf). While pesticides can ensure weed eradication, they pose a risk to human health and the environment. In this context, the early detection of weeds can allow a dramatic reduction in the amount of pesticide required. Here we present the use of edge detection techniques to identify the presence of these invasive plants in ornamental lawns and sports turf. Regarding the former, images from small experimental plots in the facilities of IMIDRA were used while images for the latter were taken on a golf course. Up to 12 different filters for edge detection were tested on the images collected. Aggregation techniques, with a range of cell values, were applied to the results of the three most effective filters (sharpening (I), sharpening (II), and Laplacian) to minimise the number of false positives. After the tests with different cell sizes, two filters were selected for more in-depth analysis. Box plots were selected to define the best cell size and identify the filter with the best performance. The sharpening (I) filter and the aggregation technique with the minimum value and a cell size of 10 offered the best results. Finally, we determined the most appropriate threshold value on the basis of the number of false positives, false negatives, and derived indexes (Precision, Recall, and F1-Score). A threshold of 78 gave the best performance. The results achieved with this methodology differed slightly between ornamental and sports turf.

Keywords: image processing, filters, golf course, ornamental turf, aggregation technique, sharpening filter

1. Introduction

Weed propagation is a major problem for golf course and ornamental turf management. These invasive plants compete with the turfgrass for sunlight, soil nutrients, water and space [1, 2]. Also, weeds can be unsightly and may affect the quality of play on golf courses [3]. Indeed, in one study, 50% of the golf players reported that they might stop using a golf course if there were too many weeds on the fairways [4]. Moreover, other authors have described that the invasion of weeds in parks and common green areas could reduce the usability of public spaces [5]. Also, the same study reported that weeds can cause seasonal erosion due to their inability to maintain a continuous surface, as it is the case with adapted turfgrass species.

Therefore, in this context, the elimination and control of weeds is essential. However, this task is difficult because weeds show faster growth than turfgrass species. Moreover, if not detected early and eradicated, weeds can spread rapidly, invading all turfgrass surfaces. Herbicides are widely used for weed control as they are easy to use and fast-acting. However, the use of significant amounts of herbicide causes environmental pollution and increases the cost of weed control [6, 7].

Furthermore, given that the citizenry comes into direct contact with both urban and sports turfgrass leisure areas, the use of chemical herbicides is discouraged. In this regard, alternatives to chemical products for weed control and removal are called for. Indeed, a weed control method that allows a reduction in the use of herbicides or a non-chemical method is preferred [7].

Technological advances seeking to ensure crop sustainability and environmental protection have brought about a decrease in the use of chemical herbicides. In this context, considerable research effort is being channelled into systems that allow a further reduction of herbicide use, thereby decreasing water contamination and the damaging effects caused by these chemicals on the environment [8, 9]. Remote sensing techniques and sensors have emerged as effective approaches for the early detection and precise identification of weed species. In this regard, digital imagery can capture images of a grass surface and process them to identify distinct compositions. In the context of weeds, this technique analyses the images in two stages, first by the segmentation of vegetation against the background (soil and harvest remnants) and second by the detection of the vegetation pixels that represent these invasive plants [10]. Moreover, the segmentation of vegetation usually assumes that all pixels corresponding to vegetation can be easily extracted by a combination of the colour planes on the RGB (red, green, blue) bands [8, 11]. In some cases, a combination of pixel values in each of the bands can be used [12], while in others the method selected was the boundary detection tool [13, 10].

After identification of vegetation pixels, weed detection by processing methods is usually achieved by merging information on the differences in colour, form, texture, position and size and spectrum of weeds and crop [10]. Moreover, a study in a corn crop described a computer vision system that can be used with videos [10]. Those authors checked the effectiveness of their system under different light conditions and informed that it detects 95% of weeds and 80% of crops. Another image processing methodology for weed detection used colour to differentiate between soil and grass [14]. The resulting image was then converted to a grayscale image to apply an edge detection technique. Afterwards, the image derived from edge detection was divided into 25 blocks, and the analysis of each block determined whether it contained narrow leaves of weeds, broad leaves of weeds, or crops. Furthermore, the use of ultra-high resolution aerial images to detect intra-row and inter-row weeds has been described [15]. In that study, the authors used semi-automatic object-based image analysis with randomly chosen forests. Also, they used the aforementioned techniques to classify soil, weeds, and crops. They applied this approach to corn crop fields and reported that it gave excellent results, but that it required powerful software to perform target recognition. Several studies have applied simple image processing techniques to turfgrass [16, 17, and 13]. Image processing was used to detect turf cover on lawns [16, 17]. In those studies, they worked with the histograms of the grass images to determine the weight of the grass and the level of coverage (high, low, very low). Subsequently, they showed the use of a new form of weed detection based on photographs taken from drones. In this case, a combination of the pixel values in the RGB bands was used to distinguish different types of cover (soil, grass and weed), and their results offered different formulas depending on the needs, with different percentages of false positives and false negatives [13].

Here we present the use of digital images and processing as a low-cost and straightforward technique for the early detection of weeds in turfgrass , thereby allowing early measures to be adopted to prevent their rapid propagation in all turfgrass surfaces and thus facilitating real-time control and treatment. This paper proposes an optimal combination of edge detection and post-processing techniques to identify, with a threshold value, weed and turfgrass presence. A series of pictures were used to test the suitability of the proposed methodology and to select the most effective filter for edge detection. Various grass species, including *Agropyron cristatum, Cynodon dactylon, Lolium hybridum, Poa annua, Agrostis stolonifera, Festuca arundinacea*, and *Agrostis stolonifera*, were photographed in two locations. In all cases, the turfgrass was composed of two grass species. Although *Poa annua* can be considered a weed, in this paper we focused on the detection of dicotyledonous species. First, we tested up to 12 different filters for edge detection and compared their performance. Of these filters, we selected the three with the most promising results. Next, we evaluated various post-processing options, including different cell sizes for aggregation techniques

and distinct mathematical operators. Finally, we used new images to test the best threshold value using different indexes that take into account false positives and false negatives.

2. Materials and Methods

2.1. Selected location

To test our proposal, we selected two locations with lawns with a uniform appearance and holding different grass combinations. Also, the selected locations had tall and short grass coverage, thereby covering distinct field scenarios.

The first location was "El Encín", the experimental area of the IMIDRA laboratories. This area holds experimental plots, each measuring 1.5 m², used to evaluate the performance of different grass combinations under water stress conditions. However, the grass coverage is low in some of the plots due to reduced irrigation. These plots were used to test the different methodologies for edge detection. We used pictures of areas with high and low grass coverage and with and without weed presence.

Furthermore, we sought to evaluate the performance of the proposed method in a real scenario. In this regard, we selected a second location, "Encín Golf", a golf course located 1 km away from the experimental plots. The golf course has several differentiated areas, including different grass species, different mowing patterns, and a low presence of weeds. However, weeds have appeared in some areas of the golf course. We took pictures of these areas, which include teeing areas, greens, and the fairway, among others. The location of the two sites is shown in Figure 1.

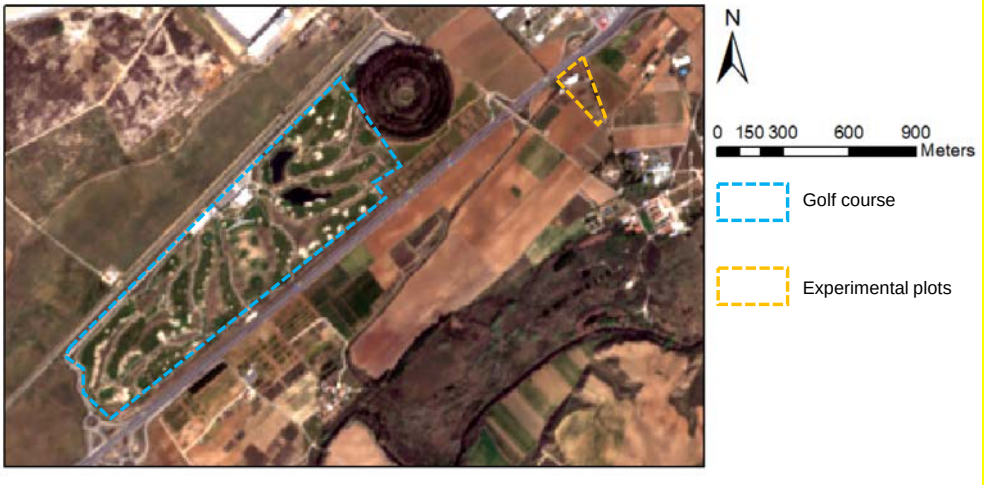

Figure 1 Location of the two areas used to obtain the pictures used in this study.

2.2. Species included

We included different species of turfgrass and weeds. For the former, we took pictures of ornamental and sports turfgrass. Among the ornamental turfgrass, C3 and C4 species were analysed to develop a methodology that is not affected by the predominant species in the turfgrass. In the sports turfgrass, C3 grass species were examined. Table 1 provides details of the pictures used, details of grass and weed species, as well as location.

2.3. Equipment used to take the pictures

We used two types of camera to ensure that the application of the methodology regardless of the origin of the images in terms of camera.

To collect the pictures at the experimental plots of IMIDRA, a Sony DSC-W120 digital camera was used. This camera has a Super HAD CCD sensor. The pictures obtained had a resolution of 7.2 megapixels (MP). More details of this camera can be found in Table 2. For pictures of the golf course, we used a Canon EOS 77D digital single-lens reflex camera. This device has a CMOS sensor of 22.3 x

14.9 mm that gives a picture of 24.20 effective MP. The features of this camera are shown in Table 1. The distance between the camera and the grass was also another variable. While in the experimental plots all the pictures were taken from a height of 1.5 m, the height varied from 1 to 1.5 m for pictures of the golf course. These heights were chosen to ensure the capture of the entire experimental plot in a single picture while maintaining a high resolution. In addition, 1.5 m is the height at which other pictures used in previous papers were gathered [13].

Table 1. Detaills of species included

Id	Grass Species	Weed Species	Type	Location
(0)	*Agropyron cristatum* *Cynodon dactylon*	*Malva sylvestris* *Diplotaxis erucoides*	Ornamental	Experimental plot
A	*Lolium hybridum* *Poa annua*	*Diplotaxis erucoides*	Sports	Fairway
B	*Agrostis stolonifera* *Poa annua*	*Centaurea sp.*	Sports	Green area
C	*Agrostis stolonifera* *Poa annua*	*Centaurea sp.*	Sports	Green area
D	*Lolium hybridum* *Festuca arundinacea*	*Malva sylvestris* *Taraxacum officinale* *Centaurea sp.*	Ornamental	Outrough area
E	*Agrostis stolonifera* *Poa annua*	*Daucus carota*	Sports	Green area

Table 2. Characteristics of cameras used.

Characteristics	Camera used at IMIDRA	Camera used at golf course
Commercial name	Sony DSC-W120 [14]	Canon EOS 77D [15]
Size of the picture	2048x1536 pixels	6000 × 4000 pixels
Horizontal and vertical resolution	72 ppp	72 ppp
Bit Depth	24	24
F point	f/7.1	f/7.1
Focal distance	5 mm	18 mm
Exposure time	1/400 s	1/250 s
ISO Velocity	ISO - 125	ISO - 100

2.4 Methodology

2.3.1. Pre-processing

Pre-processing steps involved the reduction of picture-size and the extraction of grass images. The former was carried out only for the evaluation of the method and was not used in true field conditions. The reduction of picture size allowed for easier evaluation of the results and reduced the number of processed data. Moreover, it allowed us to remove parts of the pictures showing other surfaces, such as tarpaulins. Therefore, not all pictures were the same size.

The second step, namely the extraction of grass images, was performed when the method was implemented in true field conditions, at the golf course. The aim of this step was again to reduce the amount of processed data. We used an equation described in [13], which allowed extraction of only the green grass from the picture by combining the picture bands. Each picture was divided into three bands, also known as RGB bands.

2.3.2. Edge detection

The green grass data isolated in the photos from the pre-processing stage was used with the edge detection methods to determine the presence or absence of weeds. It is important to note that this method works with the single bands of the RGB pictures.

Edge detection aims to determine the areas (pixels) that can be defined as an edge. According to the operational principle of this technique, an edge is a pixel that has a different value to that of its neighbours in the selected band of the RGB picture. In our case, the edge represents the limits of each leaf. The higher the difference, the greater the edge, thereby indicating a significant difference between the object (a leaf in our case) and the nearby object. Several filters are used to determine where the edges are placed. The filters use a matrix to calculate the new value of the pixel, which is integrated with that of neighbour pixels. With the calculated data, a new image is created. In this new image, the areas that do not represent a change—and are therefore not edges—have low values (close to 0).

In contrast, the areas considered edges have higher values. The exact value depends on the filter selected. Given that not all filters can detect all the edges of a picture, we sought to determine the best performing filter for the detection of weeds. To this end, we hypothesised that the areas of the picture that represent grass have a high variation, which would be considered as edged in the new image. Meanwhile, the areas of the picture representing weeds would have a higher uniformity because weeds have taller leaves compared to grass and they would be represented by low values in the resulting image.

Different kinds of filters can be used to build the matrix. Most filters included in the matrix use the value of the pixel (PI) and that of its eight closest neighbours (N1, N2, ... , N8) to calculate the value assigned to the PI in the new image. Thus, most of the matrices used are 3x3.

Regarding filters, they can be divided into different groups: (i) edge detection filters (these were used to determine the areas corresponding to weeds); (ii) sharpening filter (these were used for weed detection); and (iii) smoothing filters (these were used in the post-processing).

First, with respect to edge detection filters, we focused on those most commonly used: gradient, line detection, Laplacian, and Sobel.

When the goal is to detect changes (edges) in increments of 45º, gradient filters are the most useful. In this regard, there are different matrices for different gradient filters. We used the North, East, South, and West Gradient filters, shown in Figure 2. It is important to note that each filter detects the edges in a specific direction. The gradient filters have been widely used to detect edges in remote sensing for urban areas. However, their use for the detection of uneven edges is not recommended, since the edges do not follow regular vertices or vectors.

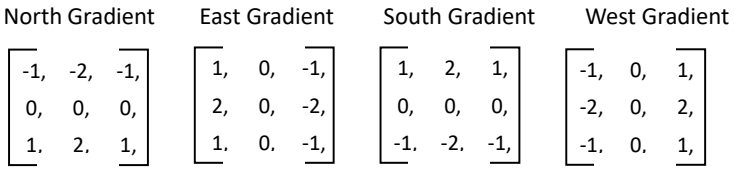

Figure 2. Gradient filters used in our study.

We used four variants of line detection filters (Figure 3). The variants differ depending on the direction of the edges that the filter highlights. Hence, the vertical line and horizontal line are the simplest filters and the left diagonal line and right diagonal line are more complex ones. Line detection filters are similar to gradient filters, in that each one is useful for detecting changes in a specific direction.

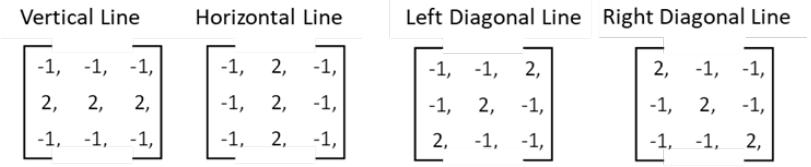

Figure 3. Line detection filters used in our study.

Regarding Laplacian filters, we used the simplest variant, which uses an operator comprising a 3x3 matrix (Figure 4). The main difference between this filter and the previous ones is that it offers the possibility to detect edges regardless of the direction or the gradient of the change.

Laplacian (3x3)

$$\begin{bmatrix} 0, & -1, & 0, \\ -1, & 4, & -1, \\ 0, & -1, & 0, \end{bmatrix}$$

Figure 4. The Laplacian filter used in our study.

Finally, regarding the Sobel filters, they are already covered by the gradient filters as some matrices are shared. To ease the nomenclature, we refer to the vertical Sobel as west gradient filter and the horizontal Sobel as north gradient filter.

Of note, all the filters can be applied individually to determine the edges of a picture. However, some filters can be used jointly to enhance edge detection. This option is particularly relevant in the case of the line detection filters and gradient filters. In this regard, we combined the two types to improve the detection of edges in different gradients and directions, thereby overcoming the main limitations of each filter. In this regard, each filter was applied individually, and the resulting image of each one was combined by simply adding the value of each pixel in each of the resulting images. This approach generated a new image that represented a combination of different filters.

Regarding the smoothing and sharpening filters, these were used in the post-processing stage. Like the other types of filter, there are many variants. We used two variants that use as operator a 3x3 matrix and one that uses a 5x5 matrix (Figure 5). These high-pass filters accentuate the comparative difference between the PI and its neighbours, as was done by the aforementioned filters.

Sharpening [3x3] (1)

$$\begin{bmatrix} -1, & -1, & -1, \\ -1, & 9, & -1, \\ -1, & -1, & -1, \end{bmatrix}$$

Sharpening [3x3] (2)

$$\begin{bmatrix} -0.25, & -0.25, & -0.25, \\ -0.25, & 3, & -0.25, \\ -0.25, & -0.25, & -0.25, \end{bmatrix}$$

Sharpen [5x5]

$$\begin{bmatrix} -1, & -3, & -4, & -3, & -1, \\ -3, & 0, & 6, & 0, & -3, \\ -4, & 6, & 21, & 6, & -4, \\ -3, & 0, & 6, & 0, & -3, \\ -1, & -3, & -4, & -3, & -1, \end{bmatrix}$$

Figure 5. Sharpening filters used in our study.

2.3.3. Post-processing

To ensure that the areas classified as weed truly corresponded to weed leaves and not to other surfaces, we used an aggregation technique to reduce the number of false positives.

Aggregation techniques allow the value of a single pixel to be combined with that of its neighbours. Also, they increase the size of the pixel. The new pixel has a value and a size that is calculated according to the selected tool. When defining the tool to be used, the size of the resulting pixels, as well as the mathematical operator used to calculate the value of these new pixels must be selected. A mathematical operator such as maximum, minimum, mean, median, or even the summation of the pixels can be used. The size of the new pixels will affect the number of neighbours to be combined. The bigger the cell or size of the new pixel, the higher the number of pixels that will be combined in the mathematical operator.

The operator selected will depend on the purpose. As our intention was to detect the areas where a group of pixels presented a low value, those mathematical operators that maximise the higher values to avoid false positives were required. Therefore, we chose the maximum and the summation as mathematical operators. Regarding cell size, we considered the following values: 3, 5,

and 10. Figure 6 provides an example of the operation principle of this aggregation technique in the case of a cell size of 3. In this figure, we include a portion of the picture of 9x9 pixels, as a detailed example, and a more significant portion of one of the pictures used in this study (Picture A), and the results of applying the aggregation technique of summation and maximum operators.

Once the aggregation technique had been applied, we grouped the pixels of the resulting image into two categories: weed (or positive detection) and grass (or negative detection). Various approaches can be used to classify pixels. In previous work, we reported the benefits of statistical parameters to create classes when the lighting conditions change. Other options include the use of natural breaks, also known as Jenks, or a threshold value based on the preliminary results.

The block diagram shown in Figure 7 shows the steps of our methodology, from the attainment of the bands to the classification.

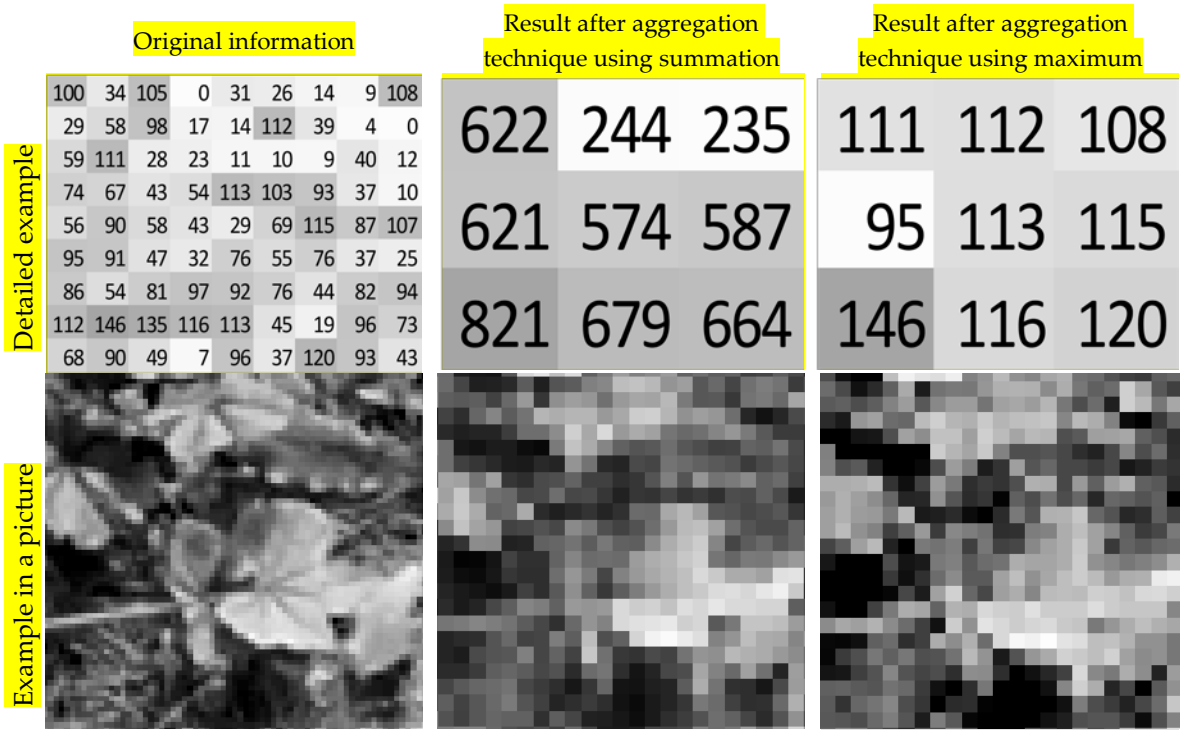

Figure 6. Differences between aggregation techniques with fixed cell size and two mathematical operators.

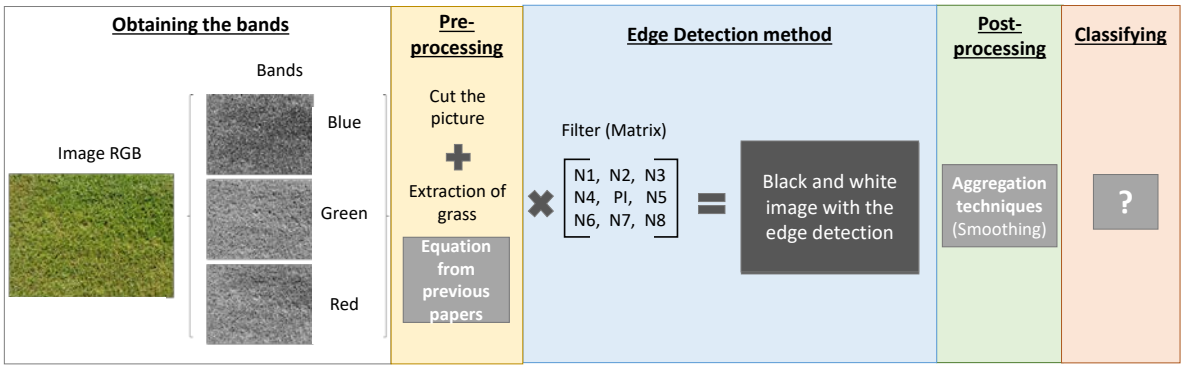

Figure 7. Representation of the different steps.

3.1. Comparison of filters

We first selected two of the pictures to evaluate the performance of the selected filters. The pictures were of areas with weed presence, and each one was taken in different light conditions (different day and hour). Furthermore, the first picture, taken at the experimental plots, presented several areas with low coverage or no grass coverage. In contrast, the second picture, taken at the

golf course, presented very high grass coverage. Thus, the comparison of filters offered us results in different scenarios and ensures that our method can be applied regardless of grass coverage.

To check the performance of filters, we examined their capacity to differentiate leaf edges. The raw data (the RGB composition) and the equation to extract the grass were used in conjunction with the filters. Figures 8 and 9 show the results of the filters for the two pictures. The red circles indicate the exact location of the weeds. The figures contains the entire picture used as the RGB composition, the RGB composition without the soil, the Red Band without soil, and the results of the application of filters. The RGB composition reveals the weed and the grass. We include a zoom of the first three images (RGB compositions and the red band) to allow better visualisation.

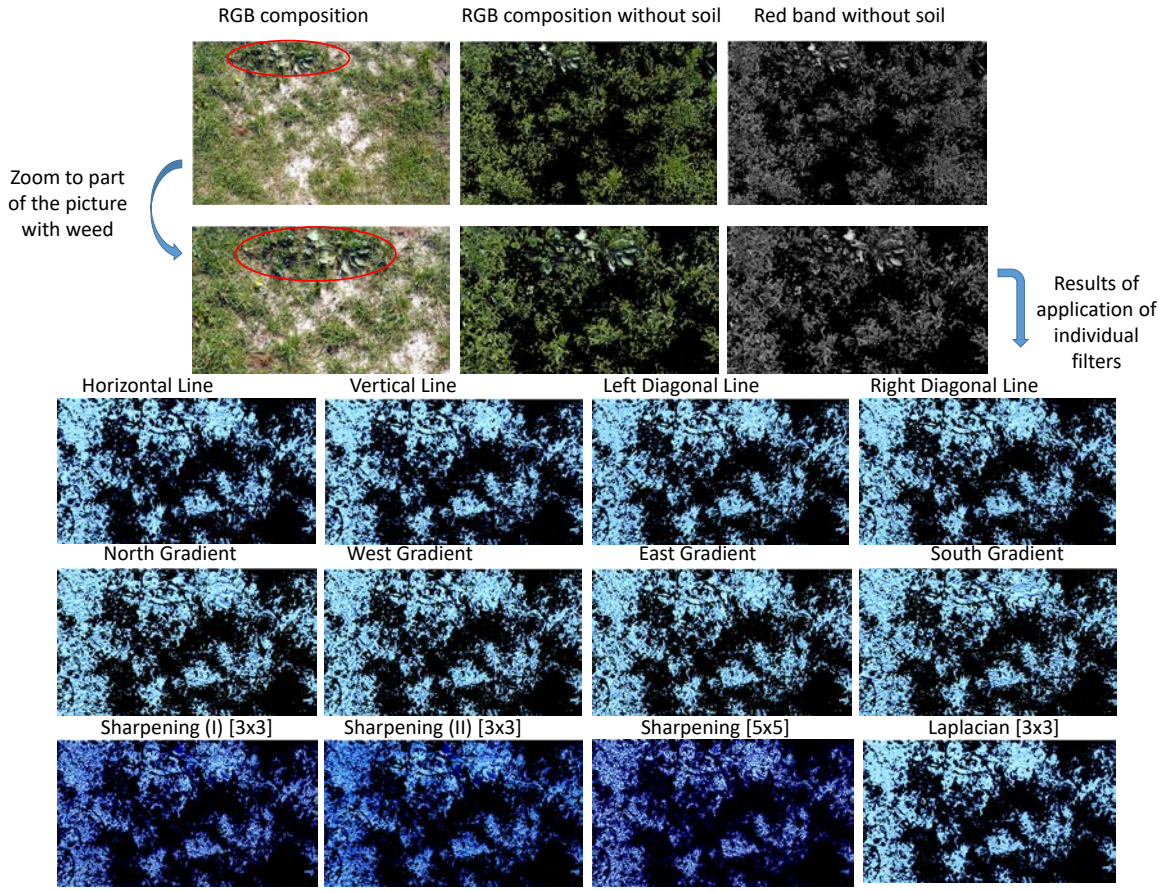

Figure 8. Results of the application of the filters in images taken in the research facilities.

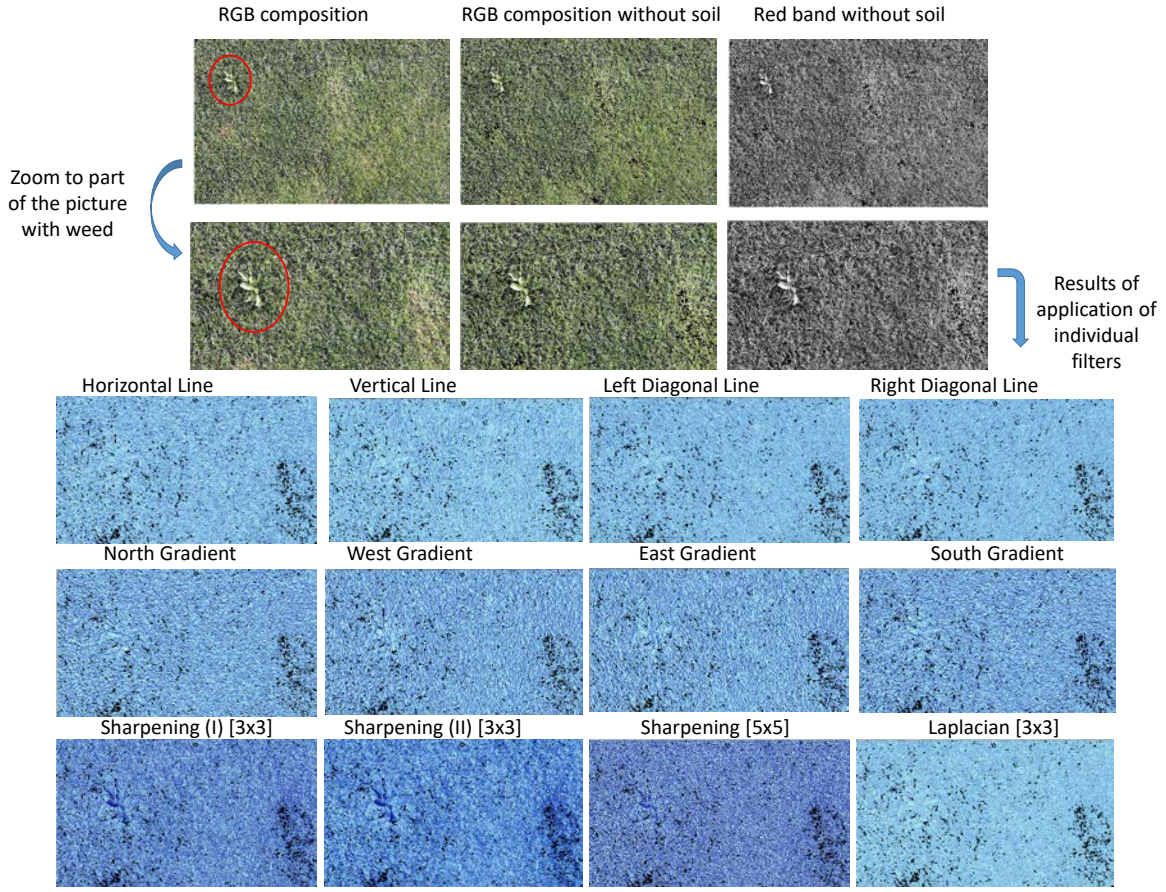

Figure 9. Results of the application of the filters in images taken at the golf course

The results indicate that the gradient filters are not useful for weed detection since they discerned changes in only one direction. The same results were found when using the line detection filters. The Laplacian filter appeared to give better results since the areas that represented the broad leaves of weed species were characterised by low values. In contrast, the results of the sharpening filters proved that capacity to detect weed, but not in an expected way. The pixels that represented weed leaves had higher values than the rest. We hypothesised that, after the application of filters, the areas with profound changes (the broadleaves of weed species) would have low values, and that an aggregation technique such as summation or maximum would allow us to identify those leaves. Therefore, to use the outputs of the sharpening filters, another aggregation technique was required.

Having confirmed that the Laplacian and the sharpening filters gave excellent results in the pictures taken, we examined their effectiveness in pictures of different areas of the golf course, including fairway, green and outrough. The purpose of this step was to ensure that the filters could be used regardless of the intrinsic characteristics of each area. Of note, the grass characteristics of each of these areas, including the species and grass height, differed, as did the presence of weed species (due to distinct maintenance practices). Figure 10 presents the results of the filters that offer the best chances of detection in Figures 8 and 9 in Pictures A) to D). Figure 10 includes four images of weeds detected in the golf course: image A) corresponds to the fairway, B) and C) to green areas and D) to the outrough. As in the previous figures, the soil and dead leaves were extracted from the picture, and only the green leaves are shown. In addition, the weeds are indicated with a red circle. The results of the Laplacian filters show that the areas representing weed leaves have a lighter colour. In contrast in the sharpening filters, the weed leaves are indicated in a darker colour. Despite excellent performance of these two types of filter in detecting weeds, several grass leaves were marked with colours similar to those corresponding to weeds. Therefore, as expected, we had to apply a post-processing aggregation method to downplay the number of false positives.

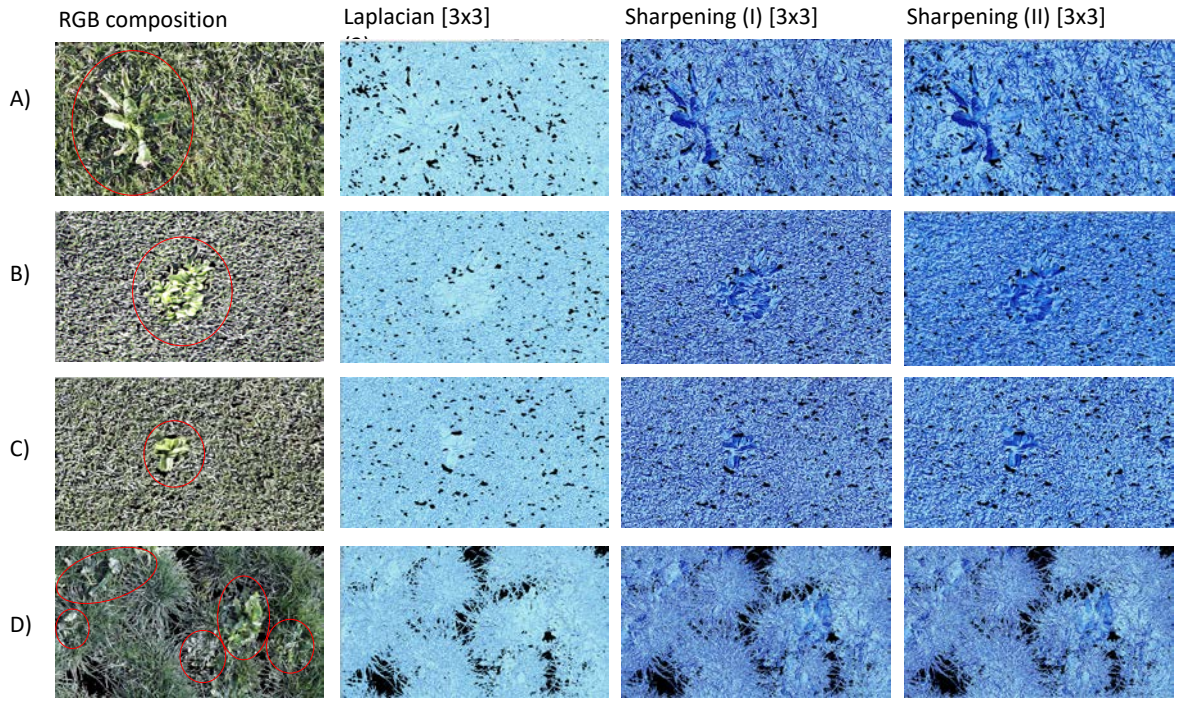

Figure 10. Results of the selected filters in four images representing different areas of the golf course (A) fairway, B) and C) greens and D) outrough).

3.2. Evaluation of aggregation techniques

In this subsection, we identify the threshold value that can be considered as positive detection and define the correct parameters for the aggregation technique. The aggregation technique used for the Laplacian and sharpening filters differed. For the former, we used the maximum value and for the latter the minimum value.

Of note, the use of the Laplacian filter with an aggregation technique has been found to be useful for identifying weed plants [18]. In that study, the authors proposed a threshold of 18 as a suitable limit with proper illumination. Since our pictures were taken in similar environmental conditions, we applied this threshold and evaluated its suitability. However, given the lack of information regarding a threshold for the two sharpening filters, we assessed convenient threshold values for the three selected filters. To this end, we divided each picture into 12 subpictures and obtained the statistical information of the pixels in each one. Next, we used the data obtained, including the minimum, maximum, and mean value, to define the threshold for each filter. With regards to the aggregation technique, we considered the maximum value for the Laplacian filter and the minimum value for the two sharpening filters. These mathematical operators were selected to reduce the number of false positives by smoothing the data.

First, Picture C was used to compare was used to compare the performance of the three filters, without taking into account any threshold value. The data of each of the 12 subpictures is shown in Figure 11, which indicates the maximum (Max) value of the pixel in each one subpictures for the sharpening (I) and (II) filters and the minimum value for the Laplacian filter. The weed plant is shown in subpicture 8. We first sought to determine whether the filters could identify this weed. To this end, we compared the value (Max or Min) obtained with each filter in subpicture 8 with the other subpictures. When the cell size was equal to 3, the values provided by the filters were similar for each subpicture. We therefore concluded that this cell size was not useful. For a cell size of 5, the results of the sharpening (I) filter continued to be similar; however, the higher maximum pixel value, were found for subpictures 5, 8 10 and 11.

In contrast, when the sharpening (II) filter was used, the maximum pixel values were found in subpictures 4, 8, 10 and 11. In the case of the Laplacian filter, the only subpicture that gave a result

other than 0 was subpicture 5. Finally, for a cell size of 10, the sharpening (I) filter gave the highest pixel values in subpicture 8, with a maximum value of 159, followed by the subpicture 10, with a maximum value of 110. These results indicate that this combination of filter and aggregation technique is a promising option for weed identification. However, the results from the sharpening (II) filter indicates that this approach is not optimal for weed detection since the maximum value was not found in subpicture 8. Also, the results of the Laplacian filter with a cell size of 10 often gave a similar result to subpictures 3 and 8. The minimum pixel value for those subpictures was 21. This value, which can be used as a potential threshold, is higher than the threshold reported in previous papers [18].

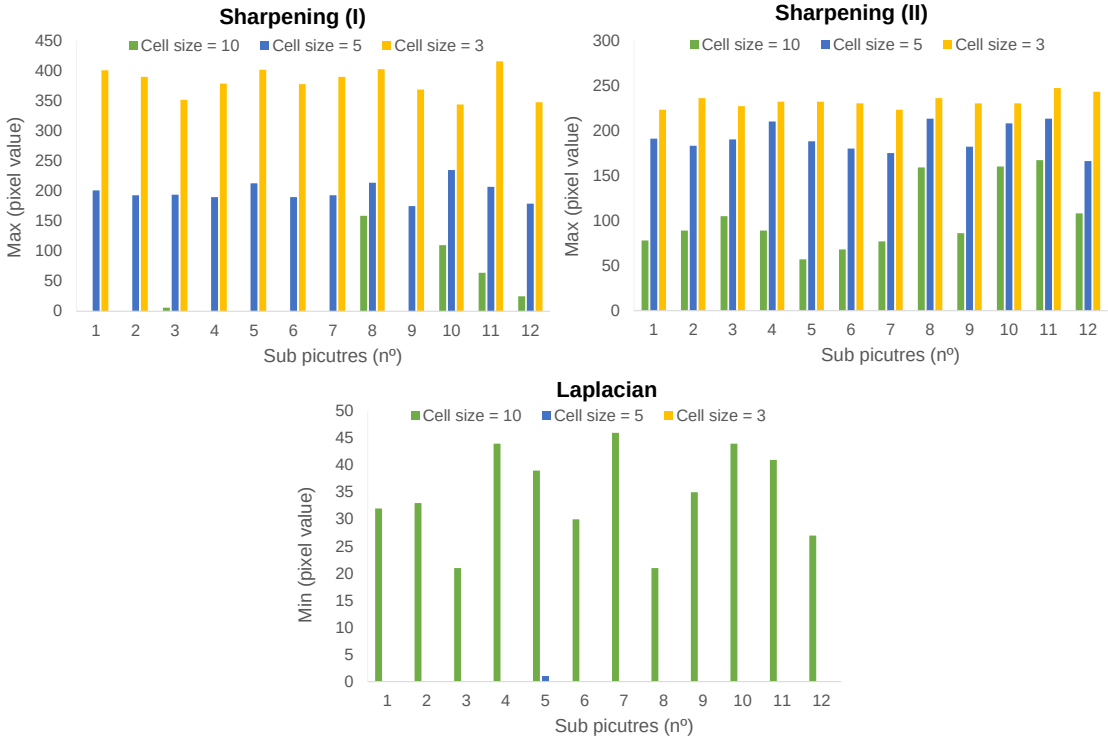

Figure 11. Maximum and minimum pixel value in each subpicture of Picture B combining different filters and cell size for the aggregation technique.

After considering the results presented in Figure 12, the sharpening (II) filter was omitted from further study. Moreover, since the results of a cell size of 3 gave similar results in all the subpictures (especially for the Laplacian filter), we focused on cell sizes of 5 and 10. On the basis of the data analysis presented in Figure 12, we provide a summary of the results of filters and cell sizes of subpictures of pictures A), B) and C) in Figure 13. We divided the subpictures into two groups, those that show the presence of weeds (WP) and those that do not (NWP). We then combined the results of pictures A) to C) according to the filter and cell size to generate a box plot for each combination of filter and cell size. Box plots are used to summarise a set of data, showing the mean, median, maximum, minimum, and outlier values. For the first plot, sharpening (I) filter and a cell size of 10, we can see that both sets of data have different maximum pixel values, thus allowing the use of this combination of filter and cell size to differentiate weeds.

However, for all the other combinations, the data from the WP and NWP subpictures showed very high similarity, thus preventing their use for weed identification. Indeed, the use of these data would give a high number of false positives, since pixels that do not correspond to weeds would have the same value as those that do. Finally, we determined the threshold to be used for weed identification. Considering the box plot, we determined that the threshold should be between the maximum value of NWP and the minimum value of WP (without considering outliers), namely 78 and 92, respectively.

3.3. Verification of the method and selection of the best threshold value

To test the weed detection performance of the method with a different threshold, we selected three thresholds, 78, 85 and 92, and applied them to two pictures from the golf course, one with high weed density (Picture D) and one with low weed density (Picture E). The pictures used are provided in Figure 12. Performance was evaluated using the following indicators: Precision (1), Recall or Sensitivity (2), and F1 Score (3). The parameters evaluated in these indicators were False Positives (FP), False Negatives (FN), and True Positives (TP).

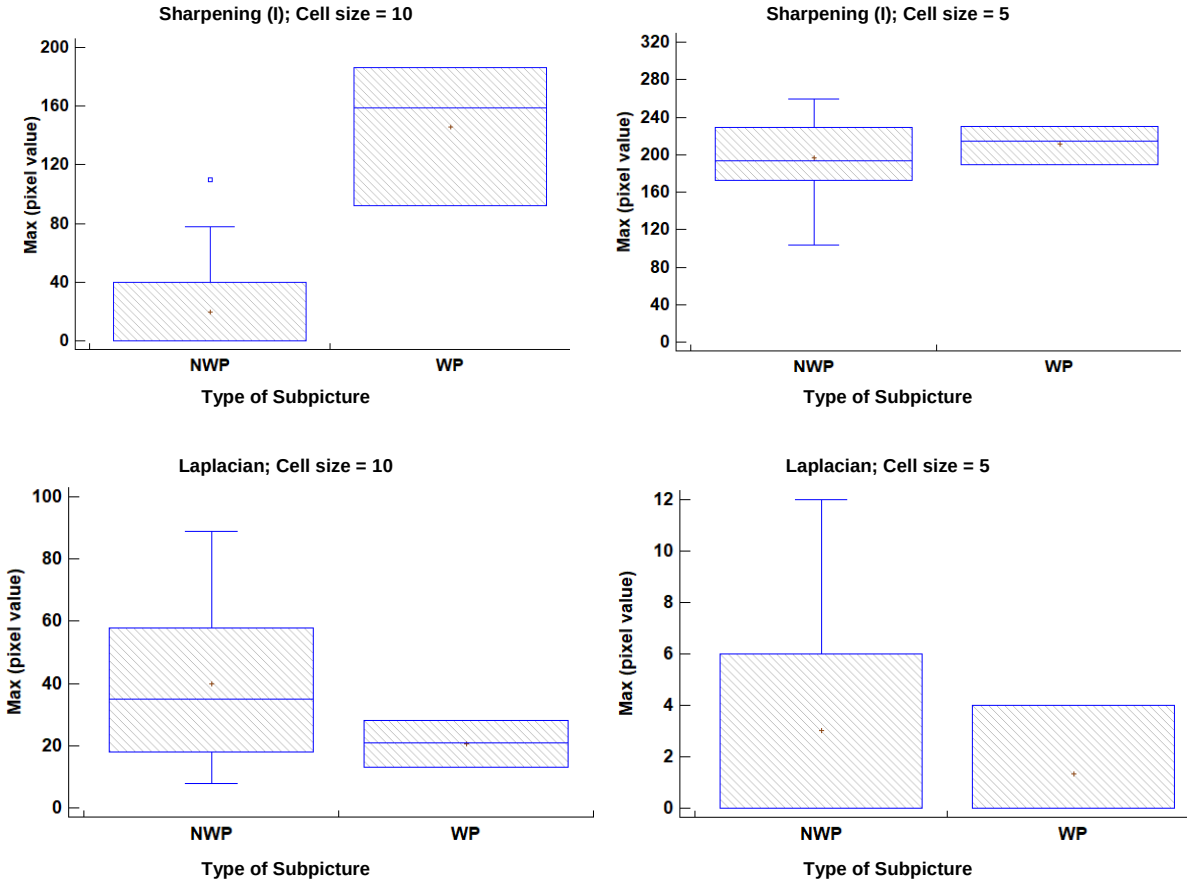

Figure 12. Box plot for each combination of filter and cell size for pictures A) to C).

We considered as FP all pixels with a value higher than the threshold which do not represent a weed leaves. The TP is the number of weeds with one or more pixels with a value above the threshold. Finally, FN refers to the plants that have no pixel with a value higher than the threshold.

The results of the validation test are summarised in Figure 14, Table 3 and Table 4. Figure 14 shows the results, focusing on Picture D) since the results are more evident in this picture. Figure 13 provides the classification of pixels considered as weeds in red in the "General results with threshold = 92".

$$Precision = TP/(TP + FP), \quad (1)$$

$$Recall = TP/(TP + FN), \quad (2)$$

$$F1\ Score = 2 \times (Recall \times Precision)/(Recall + Precision), \quad (3)$$

Figure 13. Pictures for the verification process, including the golf course and IMIDRA images with different weed densities.

Three sections of the picture were then enlarged to facilitate the identification of red pixels. We include for each one of these sections the original picture, and the results with threshold = 92 and with threshold = 72. We selected the most different thresholds in the pictures to maximise the differences. As in Figure 10, the black areas represent the soil, and those areas were not analysed since they were extracted from the picture in the pre-processing stage.

In Table 3, we outline the number of TP, FP, and FN for Pictures D) to E) considering the three proposed threshold values. The techniques developed, which are a combination of two image processing techniques, detected 24 out of 28 weeds in the image with high weed density and 6 out of 7 when the lowest threshold value was used. As the threshold value increased, the number of FN increased as the number of FP fell. To determine the best threshold, we selected the one with highest F1 Score in Table 4. The results indicate that the lowest threshold showed the highest F1 Score. Although the precision of the technique rose as the selected threshold increased, the Recall decreased dramatically.

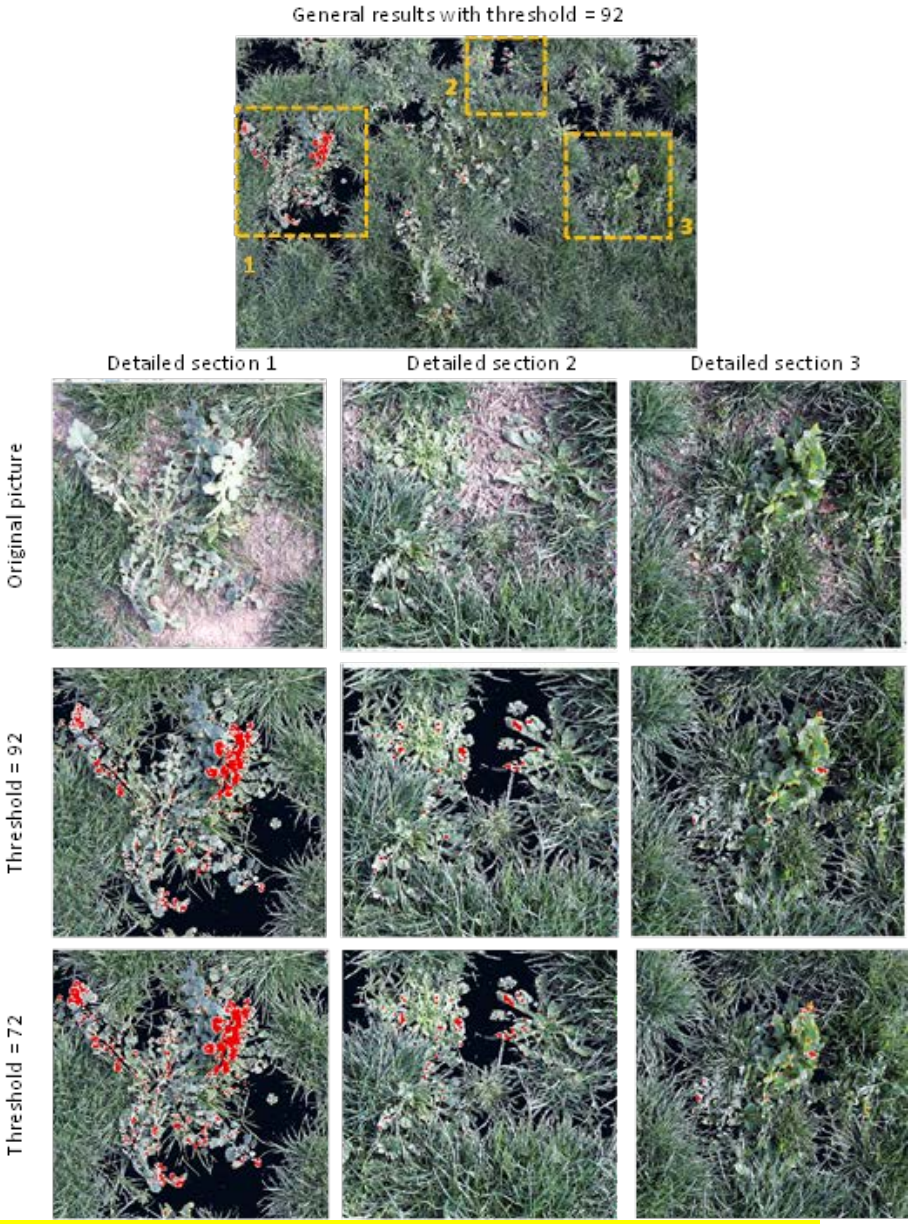

Figure 14. Summary of identification of weed plants (in red) for Picture D).

Table 3. Results of verification test in terms of FP, FN and TP.

	Threshold = 78			Threshold = 85			Threshold = 92		
	TP	**FP**	**FN**	**TP**	**TP**	**FN**	**TP**	**FP**	**FN**
Picture D)	24	6	4	19	4	9	16	3	12
Picture E)	6	3	1	5	2	2	3	1	4

Table 4. Value of Precision (Pre), Recall (Rec) and F1 Score (F1) for the different thresholds.

	Threshold = 78			Threshold = 85			Threshold = 92		
	Pre	**Rec**	**F1**	**Pre**	**Rec**	**F1**	**Pre**	**Rec**	**F1**
Picture D)	80%	86%	83%	83%	68%	75%	84%	57%	68%
Picture E)	67%	86%	75%	71%	71%	71%	75%	43%	55%

4. Discussion

4.1. Comparison of the proposed method with existing weed detection systems

The most significant advantage of the proposed method compared to existing techniques is that it can be used to detect weed species in grass. Most approaches currently used to detect weeds are applicable only to lineal crops and are not suitable for crops with uniform coverage. Several studies [18-20] have proposed the use of object detection techniques for weed detection, taking advantage of crop rows. The vegetation detected in the row was deemed the crop and that out of line was considered a weed. The high accuracy of these methods has led to their use for weed detection in lineal crops. The method proposed in [19] effectively identified weed presence in the inter-row areas of corn crops. Like the method put forward in the present paper, in [19, 20] the authors used a soil background segmentation by combining RGB bands. The average false detection rate was 4.36. In [19], the authors sought to distinguish weeds between corn rows by means of fuzzy logic and used the greenness of the pixels as the parameter to be evaluated. A series of algorithms were developed in [20] to identify weed plants in corn crops to adjust local positioning. However, the aforementioned methods are not suitable for our case study of grass since it does not follow a linear pattern.

Some studies have used artificial intelligence to detect weeds [22-25]. In this regard, the intensity of each pixel on the greyscale has been used as input for an artificial neural network (ANN) [22]. The crop in that study was corn, and different weeds were analysed, including monocotyledons and dicotyledons. This approach gave a weed detection success rate of 80%, and 62% for the different weed species. A similar study also used an ANN to distinguish between corn and weeds [23], in that case reporting 80-100% detection of corn and 60-80% detection of weeds.

In another study, computer vision was used to differentiate between sugar beet and weed (thistle) plants [24]. In that case, information from the edge-shaped and homogeneous surface detectors was merged to detect related invariant regions. The false-negative rate of this approach was under 2%. Finally, a stereovision camera has been used as input for a machine vision system [25]. In this regard, the camera was mounted on a small field robot equipped with a computer for image processing. Images were gathered at different times of the day (morning and afternoon) to ensure that the method could be used under a range of lighting conditions. The authors first used a combination of RGB bands to obtain derived products and then an Asymmetric Artificial Network (AAN) to differentiate between crops and weed. This technique achieved 90% discrimination for corn, 73.1% for tomato plants, and 68.8% for weeds.

In the future, the aforementioned detection systems are likely to have the capacity to even determine the weed species. Despite the promise of these systems, they require high power processors and in most of the cases also cloud computing techniques. Since our objective was to determine the location of weeds in real-time, or almost real-time, and then process this information, we need a method that can be applied in a drone or other vehicles able to take a picture with a limited hardware and software resources. Therefore, object recognition based on cloud computing, which requires a high computation capacity, is not appropriate for our method. Our technique can operate without high processing capacity, neither internet access.

A third type of approach has also been used for plant detection, namely hyperspectral cameras and simple techniques of pixel comparison. In this regard, sugar beet and four different weed species were identified using Euclidean distance and stepwise discriminant analysis with wavelet coefficients [26]. The tests performed in that study demonstrated that the stepwise discriminant analysis with wavelet coefficients has better discrimination capacity of plant species than most of the aforementioned systems, showing 74 and 97% success in the identification of sugar beet and the weed species respectively.

Another study proposed the use of support vector data description, a popular boundary method, to differentiate between crop and weeds [27], reporting 94.34 and 96.23% of identification accuracy, respectively. The main difference between that method and ours are the characteristics of the crop and weeds. The pictures used in that study were of soil and one plant (weed or crop), thereby facilitating the distinction of the individual shape of each plant. In contrast, we used a more

complex scenario, in which plants covered 100% of the surface in some cases. Furthermore, the selected pictures covered mixtures of grass (the crop) and weeds.

Our novel detection method (Removing soil and dead leaves + sharpening (I) filter + aggregation technique (cell size) + threshold), which was tested and verified using pictures of the golf course, including images of different areas such as the fairway, green, and outrough, allowed the identification of weeds. Moreover, the indicators of the classification system showed high values.

4.2. Implementation of our method in weed management systems

The image processing method described herein is conceived for use in weed management systems that use a drone or other vehicle to monitor grass status. Several irrigation management systems use drones to gather images to determine irrigation needs. Our weed identification technique is devised to be applied in the same vehicle that gathers these images. These vehicles are generally controlled with a simple processor unit, in which the route and picture gathering are included as algorithms. Therefore, we converted our method into an algorithm that can be included in the operational routine of the drones.

The algorithm, see Figure 15, calls the pre-established flying parameters and image capture settings according to the other algorithms included in the previous operation routine. After gathering the images, it then applies the process described in this paper (extraction of vegetation pixels, edge detection filter and aggregation technique). First, the algorithm checks whether a new image is available. Next, the code described in [19] is applied to separate the bands of the picture and operate with the red band. Once an image has been gathered and the bands have been obtained, the algorithm applies pre-processing, keeping only the pixels corresponding to vegetation and then applying the filter and aggregation technique. Next, the results are analysed to determine the presence or absence of weeds using the established threshold. When no vegetation pixels are detected, the process, including edge detection filter and aggregation technique, is not applied to the picture.

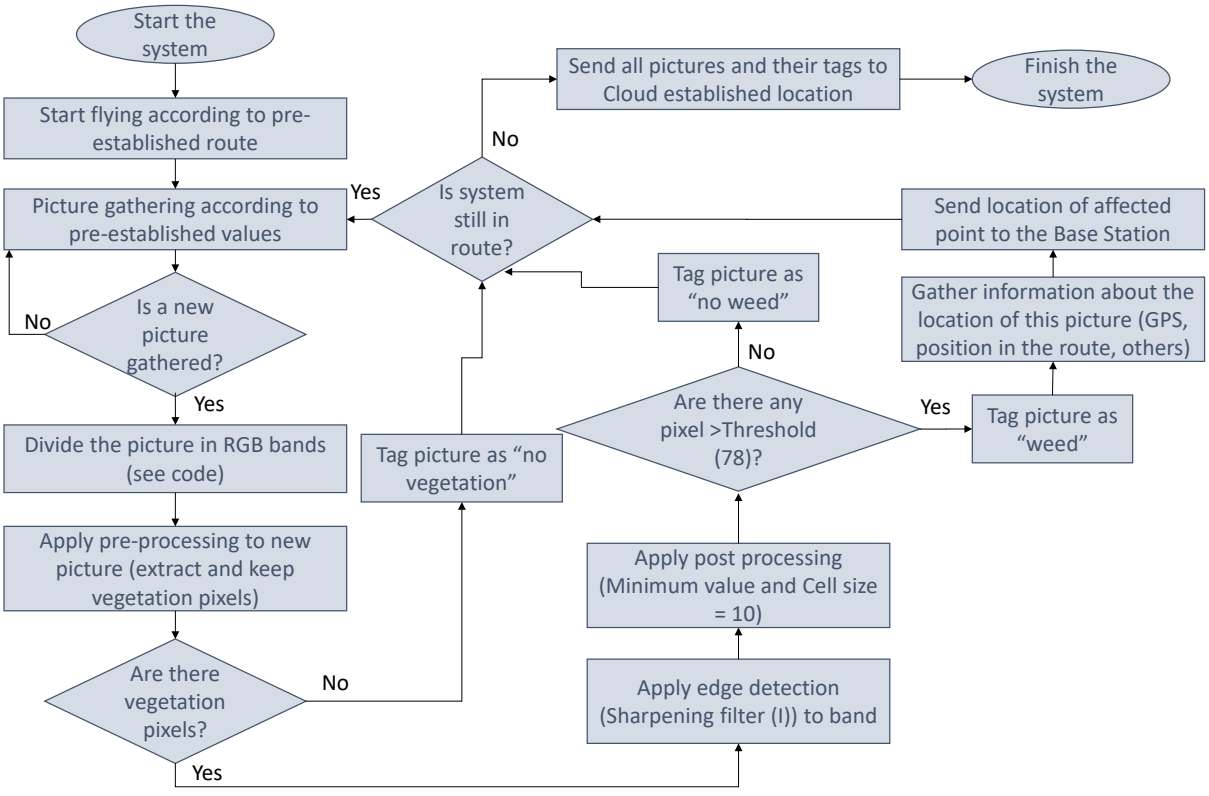

Figure 15. Operation algorithm of the proposed weed detection method in control vehicles of weed management systems.

After completion of the process, the picture is tagged as no vegetation detected ("no vegetation"), no weed detected("no weed"), or weed detected ("weed"). If the image is tagged as "weed", then the system sends the position of the picture based on the available navigation systems, which can be GPS position, the point of the established route or the time of the route. This information is then sent to a base station where a secondary vehicle, which can be operated by a person or not, will be sent to the location to start the application of the phytosanitary product. Furthermore, after the route ends, all the pictures and tags are stored in a cloud server, thereby facilitating their access for other image processing technologies that require cloud access and higher computation capacities.

Algorithm for image processing in weed detection systems has been used elsewhere [26]. Nonetheless, our algorithm includes other functions such as gathering and sending data to locate the area in which weed plants are found. Also, the algorithm proposed in [8] includes the use of AAN, which requires higher computational capacity than the method proposed herein.

Although the algorithm is proposed following the methodology described in this paper, with images gathered between 1 and 1.5 m, the results described in [19] indicates that our system can be used with data gathered from a greater height. The main limitation in this regard is the spatial resolution of the pictures obtained by the drone. Further analyses are required to establish the minimum resolution of the picture required to obtain accurate results.

The algorithm and methodology used in the present study are designed to operate with an RGB camera. However, since hyperspectral images are becoming a promising tool for precision agriculture, these images are likely to be introduced into turfgrass monitoring in the years to come. Our algorithm can be adapted to the use of other types of information, such as that provided by hyperspectral cameras, or the commonly used vegetation indexes such as Normalized Difference Vegetation Index NDVI, which include the infrared part of the spectrum. Furthermore, information calculated by other software, such as the Green Area (GA), can be included in our method in the future.

It is important to note that our method has been developed to be used under certain environmental and lighting conditions. Changes in lighting conditions during the day and at different latitudes might affect the performance of the algorithm. In other studies [28], authors have adapted existing methods to different light conditions. While the pictures used to generate the methodology described herein were taken in different periods of the year and at different times of the day, we cannot affirm that the algorithm will perform with the same precision under other lighting conditions, such as sunrise or sunset.

4.3. Differences found in the performance of the proposed method in different scenarios

To ensure that the method can be applied in different scenarios, we used pictures taken at diverse locations. Our results indicate that it performs best in uniform scenarios such as the greens and fairways of the golf course. In those areas, due to efforts in maintaining the high quality of the turf, there are no patches of soil or dead leaves. Also, continuous mowing confers the grass with a homogeneous appearance, and the only alteration in this uniformity is weed plants. However, in the outrough and ornamental grass, grass coverage is not as even as in the previously mentioned areas. The use of a pre-processing technique to remove soil and dead leaves from the images helps to minimise false positives. However, in some cases, the leaves of weed species produce shadows, which our system identifies as weeds. This is one of the most significant drawbacks of the proposed methodology. Further research should be devoted to the use of RGB band combination to avoid this problem.

On the basis of our results, we conclude that the proposed method can be used on any sort of lawn. The greater the uniformity, the better the results will be. Furthermore, turfgrass height influences the results. When the turfgrass is kept short by regular mowing, the uniformity of the grass is higher, thus facilitating the implementation of our method. In contrast, when the turfgrass is not mowed periodically (as can occur in ornamental lawns), environmental, genetic, and

management differences can lead to some individual plants having broader and more prominent leaves than others, thus altering the uniformity.

5. Conclusion

Here we have evaluated the use of an edge detection technique to identify the presence of weed plants in turfgrass. This technique is characterised by its low-cost and almost real-time operation. To ensure that applicability of our method to different types of grass, we used images from ornamental lawns and golf courses. The novelty of the proposed methodology is that it does not rely on the identification of weeds through the definition of lineal crops. It can be applied in lineal and non-lineal crops, such as the lawns. Furthermore, it is based on edge detection rather than object detection, the latter requiring high computational capacity and cloud access. Our system can be applied in devices that have hardware and software constraints and that do not need an internet connection during image processing.

The proposed method includes a pre-processing part (evaluated in previous papers [13], image processing based on edge detection, and post-processing involving an aggregation technique. The processing and post-processing were evaluated by various techniques in each step and using statistical analysis and the number of FP, FN and other indicators (such as Rec., Pre., and F1) to evaluate performance. Finally, the proposed method is shown as an algorithm, which can be included in management vehicles that take pictures of the field, like those used in precision farming for irrigation management. It is important to note that the method has been tested in two scenarios: ornamental and sports turf. The former differs from the latter in that coverage is not as high and grass height grass tends to be greater. Although our results indicate that our approach can be used in both scenarios, its performance (in terms of Pre and F1) is better in ornamental (80% and 83%) than in sports turf (67% and 75%).

Future work will involve the evaluation of the combination of the proposed method with other techniques, such as RGB band combination (as done in [18]) or the inclusion of information from hyperspectral images (as in [27]) to classify the weeds detected. Furthermore, verification of the proposed methodology under changing light conditions, as presented in [28], will be performed. In addition, a combination of previous pictures can be used to evaluate the effects of new phytosanitary treatments for resistant weeds. Finally, the use of pictures and image processing for the detection and identification of other grass disturbances caused by diseases, such as Dollar spot, Fusarium patch disease, Rhizoctonia diseases, and Take all patch infection, will be evaluated.

Author Contributions: Conceptualisation, J. M.; Methodology, LP; Field measures and sampling, J. M., GR, and S. Y.; Data curation, LP; Writing—original draft preparation, SY. and LP; Writing—review and editing, SY, J. M., LP and PVM; Supervision, PVM, JL; validation, PVM, JL, Project administration, J. M. All the authors have read and agreed to the published version of the manuscript.

Funding: This work was partially funded by the Conselleria de Educación, Cultura y Deporte through "Subvenciones para la contratación de personal investigador en fase postdoctoral", grant number APOSTD/2019/04, by the European Union through ERANETMED (Euromediterranean Cooperation through ERANET joint activities and beyond) project ERANETMED3-227 SMARTWATIR, and by the European Union with the "Fondo Europeo Agrícola de Desarrollo Rural (ERDF) – Europa invierte en zonas rurales", the MAPAMA, and Comunidad de Madrid with the IMIDRA, through the "PDR-CM 2014-2020" project number PDR18-XEROCESPED.

Conflicts of Interest: The authors declare no conflict of interest.

References

1. AjinkyaPaikekari, VrushaliGhule, Rani Meshram, V.B. Raskar. 2016. WEED DETECTION USING IMAGE PROCESSING. International Research Journal of Engineering and Technology, 3, 1220-1222
2. Christensen, S., Søgaard, H. T., Kudsk, P., Nørremark, M., Lund, I., Nadimi, E. S., &Jørgensen, R. (2009). Site-specific weed control technologies. Weed Research, 49(3), (233-241).
3. George Waters. Weeds on the Golf Course: What Every Golfer Should Know. United States of America Golf Association (USGA). Green Section, October 11, 2019.

4. Anne Mette Dahl Jensen. Playing quality on golf course. Xxx. In STERF (Scandinavian Turfgrass and Environment Research Foundation)
5. McELROY, J.S. and MARTINS, D. 2013. USE OF HERBICIDES ON TURFGRASS. Planta Daninha. 31, n. 2, p. 455-467.
6. UkritWatchareeruetai, Yoshinori Takeuchi Modified Lawn Weed Detection: Utilisation of Edge-Color Based SVM and Grass-Model Based Blob Inspection Filterbank. Conference Paper in Lecture Notes in Computer Science. November 2007. DOI: 10.1007/978-3-540-69162-4_4 · Source: DBLP
7. UkritWatchareeruetai, Yoshinori Takeuchi. 2006 Computer Vision Based Methods for Detecting Weeds in Lawns Machine Vision and Applications, vol.17, no.5, pp.287-296
8. Yang, C, Prasher, S., Landry, J., HS, R., 2003. Development of an image processing system and a fuzzy algorithm for site-specific herbicide applications. Precis. Agr. 4,5-18.
9. ReihanehLoni, Mohammad Loghavi, and Abbas Jafari. 2014. Design, Development and Evaluation of Targeted Discrete-Flame Weeding for Inter-row Weed Control Using Machine Vision. American Journal of Agricultural Science and Technology, 2, 7-30.
10. Burgos-Artizzu, X. P., Ribeiro, A., Guijarro, M., & Pajares, G. (2011). Real-time image processing for crop/weed discrimination in maize fields. Computers and Electronics in Agriculture, 75(2), (337-346).
11. Ribeiro, A., Fernández-Quintanilla, C, Barroso, J., García-Alegre, M.C., 2005. Development of an image analysis system for estimation of weed. In: Proceedings 5th European Conf. On Precision Agriculture (5ECPA), pp. 169-174.
12. Chauhan, B. S., & Johnson, D. E. (2011). Row spacing and weed control timing affect yield of aerobic rice. Field CropsResearch, 121(2), (226-231).
13. Parra, L., Torices, V., Marín, J., Mauri, P.V., Lloret, J. (2019). The Use of Image Processing Techniques for Detection of Weed in Lawns. Proccedings of the Fourteenth International Conference on Systems (ICONS 2019), Valencia, Spain, 24-28 March, 2019.
14. Manual of DSC-W120 Camera. Available at: https://www.sony.com/electronics/support/res/manuals/3700/37007771M.pdf. Last access 10/07/2020
15. Manual of Canon EOS 77D Camera. Available at: https://gdlp01.c-wss.com/gds/3/0300026603/01/EOS_77D_Instruction_Manual_EN.pdf. Last access on: 10/07/2020
16. Paikekari, A., Ghule, V., Meshram, R., Raskar, V. B. (2016). Weed detection using image processing. International Research Journal of Engineering and Technology (IRJET), 3(3), (1220-1222)
17. Gao, J., Liao, W., Nuyttens, D., Lootens, P., Vangeyte, J., Pižurica, A., ...&Pieters, J. G. (2018). Fusion of pixel and object-based features for weed mapping using unmanned aerial vehicle imagery. International journal of appliedearthobservation and geoinformation, 67, (43-53).
18. Marín Peira, J. F., Rocher, J., Parra, L., Plaza, A., Mauri, P. V., Ruiz Fernández, J., Sendra, S., Lloret, J. (2017). Automation in the characterization of the cultivation of lawns in urban grasslands", Proccedings of the IX CongressoIbérico de Agroengenharia, Braganza, Portugal, 4 – 9 Sept. 2017.
19. Marín, J., Parra, L., Rocher, J., Sendra, S., Lloret, J., Mauri, P. V., & Masaguer, A. (2018). Urban Lawn Monitoring in Smart City Environments. Journal of Sensors, 2018 (1-16).
20. Parra, L., Parra, M., Torices, V., Marín, J., Mauri, P. V., Lloret, J. (2019). Comparison of Single Image Processing Techniques and Their Combination for Detection of Weed in Lawns. International Journal on Advances in Intelligent Systems, 12, 4, 177-190.
21. Wu, X., Xu, W., Song, Y., &Cai, M. (2011). A detection method of weed in wheat field on machine vision. Procedia Engineering, 15, 1998-2003.
22. Yang, C. C., Prasher, S. O., Landry, J. A., Perret, J., &Ramaswamy, H. S. (2000). Recognition of weeds with image processing and their use with fuzzy logic for precision farming. Canadian Agricultural Engineering, 42(4), 195-200.
23. Fontaine, V., & Crowe, T. G. (2006). Development of line-detection algorithms for local positioning in densely seeded crops. Canadian Biosystems Engineering, 48, 7.
24. Yang, C. C., Prasher, S. O., & Landry, J. A. (2002). Weed recognition in corn fields using back-propagation neural network models. Canadian Biosystems Engineering, 44, 7-15.
25. Yang, C. C., Prasher, S. O., Landry, J. A., & DiTommaso, A. (2000). Application of artificial neural networks in image recognition and classification of crop and weeds. Canadian agricultural engineering, 42(3), 147-152.

26. Kazmi, W., Garcia-Ruiz, F., Nielsen, J., Rasmussen, J., & Andersen, H. J. (2015). Exploiting affine invariant regions and leaf edge shapes for weed detection. Computers and Electronics in Agriculture, 118, 290-299.
27. Okamoto, H., Murata, T., Kataoka, T., & HATA, S. I. (2007). Plant classification for weed detection using hyperspectral imaging with wavelet analysis. Weed Biology and Management, 7(1), 31-37.
28. Jeon, H. Y., Tian, L. F., & Zhu, H. (2011). Robust crop and weed segmentation under uncontrolled outdoor illumination. Sensors, 11(6), 6270-6283.
29. Liu, X., Li, M., Sun, Y., &Deng, X. (2010). Support vector data description for weed/corn image recognition. Journal of Food, Agriculture and Environment, 8(1), 214-219.